Mathematical Biosciences and Engineering

https://www.aimspress.com/journal/mbe

MBE, 22(6): 1364–1381.
DOI: 10.3934/mbe.2025051
Received: 31 January 2025
Revised: 10 April 2025
Accepted: 18 April 2025
Published: 28 April 2025

Research article

Dynamic interaction between transmission, within-host dynamics and mosquito density

Mayra Núñez-López[1,*], Jocelyn A. Castro-Echeverría[2,3] and Jorge X. Velasco-Hernández[2]

[1] Department of Mathematics, ITAM Río Hondo 1, Ciudad de México 01080, México

[2] Instituto de Matemáticas, UNAM, Boulevard Juriquilla No. 3001, Juriquilla Querétaro 76230, México

[3] Tecnologico de Monterrey, School of Engineering and Science, Blvd. Enrique Mazón López 965, Hermosillo, Sonora 83000, México

* **Correspondence:** Email: mayra.nunez@itam.mx.

Abstract: The central question in this paper is the character and role of the within-host and between-host interactions in vector-transmitted diseases compared to environmental-transmitted diseases. In vector-transmitted diseases, the environmental stage becomes the vector population. We link an epidemiological model for a vector-transmitted disease with a simple immunological process: the effective transmission rate from host to vector, modeled as a function of the infected cell level within the host, and a virus inoculation term that depends on the abundance of infected mosquitoes. We explore the role of infectivity (defined as the number of host target cells infected), recovery rate, and viral clearance rate in the coupled dynamics of these systems. As expected, the conditions for a disease outbreak require the average individual in the population to have an active (within-host) viral infection. However, the outbreak's nature, duration, and dynamic characteristics depend on the intensity of the within-host infection and the nature of the mosquito transmission capacity. Through the model, we establish inter-relations between the infectivity, host recovery rate, viral clearance rate, and different dynamic behavior patterns at the population level.

Keywords: dengue transmission; multiple time scales; within-host dynamics; between-host dynamics; reproduction number

1. Introduction

Our previous work on the dynamics of within-host and between-host models was centered on diseases where transmission passes through an environmental stage [1–3]. *Toxoplasma gondii* is the

exemplary case. The disease cycle involves primary hosts, such as cats, where the pathogen can reproduce. The primary infected host either defecates or urinates in the environment that receives the infection stage of the pathogen, namely oocysts, from which the secondary host will acquire the disease [4]. The central question in this paper is the character and role of the intermediate stage and the environment when dealing with vector-transmitted diseases. In these diseases, the environmental stage is one of the hosts, namely the vector population. Then, the infected vector transmits the pathogen to the mammalian host. This paper compares these two kinds of disease transmission and pathogen life cycles.

The infectious disease dynamics integrate two key processes in host-parasite interactions: one is the epidemiological process associated with disease transmission, and the other is the immunological process of infection at the individual host level. The transmission of an infectious agent in a population involves various spatial and temporal scales, which are broken down into two major groups of phenomena: those that occur at the population scale (epidemic outbreaks), and those within the host (pathogen-immune system interactions). A multiplicity of papers of a theoretical nature have explored this interface, (e.g., [1–3, 5–8]). The vast majority of these works focus their analyses on directly transmitted diseases based on Kermack-McKendrick type models [9], although some studies have addressed vector-borne diseases [10, 11] but with a greater level of detail and complexity regarding the biological mechanisms involved. In [12], the author presented an age-since-infection-structured model that showed the within-host immune-virus dynamics and within-vector viral kinetics, with feedback at different levels. For example, [13] utilized a widely used model for theoretical purposes at the immune system level, which was developed for HIV to solely differentiate between the target cells, infected target cells, and virions. In particular, [1–3] have looked at the problem of the interplay of between-host and within-host dynamics in an environmentally driven disease.

Feng et al. [3], generalized their results by introducing a disease-induced death rate into the host infected class. In particular, in this setting, the evolution of virulence in the host population will favor a maximum level of virulence (at the between-host level) if the virion production at the cellular level (within-host) is maximal; alternatively, it will favor an intermediate level of virulence if the maximum rate of virion production is significant. In our model, we refer to a specific scenario where the increase in virion production (within-host replication) directly enhances the transmission at the between-host level. This is a classical assumption based on the idea that higher viral loads often correlate with: a higher probability of infecting vectors during a blood meal and an increased likelihood that the infected vector becomes infectious and transmits the pathogen to a new host. According to the above assumption and the role of time scales, the within-host dynamics (virion production, immune response, and cell infection) occur on a faster time scale than the epidemiological (between-host) dynamics.

The increase in disease-induced mortality due to higher virulence happens at a sufficiently slower rate than viral replication and transmission, thus allowing the pathogen to achieve multiple transmission events before the host dies. This separation of time scales is a common simplifying assumption in multi-scale models of infectious diseases [5, 7].

In our model, we assume that the vector infectivity depends on the viral load of the vertebrate host at the time of the mosquito bite. This approach allows us to capture the effect of the within-host viral dynamics on transmission without explicitly modeling the fate of the virus inside the mosquito. Empirical studies have shown that the probability of mosquito infection and the subsequent transmissibility increases with the host viremia [14–16], thus providing a biological basis for this assumption. Fur-

thermore, modeling frameworks such as those in [10] demonstrate that such simplifications can yield accurate transmission dynamics without sacrificing biological realism.

This paper explores the between-host and within-host trade-offs in the context of vector-borne disease in a vertebrate host. The aim of this article is theoretical. We explore the coupled dynamics of within- and between-host dynamics in vector-host transmission systems to identify the association between the within-host and between-host time scales and dynamics. As mentioned above, [2, 3] studied the interaction of these in an infectious disease with an environmental component. Through this component, the virus, is inoculated in the host when interacting with the contaminated environment, thus linking transmission at the population level with infection at the individual level. Here, we explore the same problem but replace the passive interaction between a contaminated environment and a host with that of an insect vector that actively seeks and infects the host. We restrict ourselves to infections in a mammalian host and do not consider the within-vector dynamics.

Vector-borne diseases are a group of diseases of great human importance, with nearly half of the world's population infected with at least one type of vector-borne pathogen [17, 18]. To mention just a few examples, diseases such as African trypanosomiasis, Chagas disease, and dengue fever, are serious public health problems in many regions of the world, thereby generating high levels of mortality and morbidity in at-risk populations, which are generally those with the least economic resources and with the least access to adequate public health systems [19]. On the other hand, arthropod-borne diseases are abundant in vertebrates such as horses, cattle, and other mammals. Climate change directly impacts arthropod vectors (abundance, geographical distribution, and vectorial capacity) [20, 21], thus producing a reemergence of many infectious diseases in humans and animals of direct economic importance.

We explore the fundamental relationship between reproductive numbers at the population and individual levels, particularly the role of the within- and between-host systems in epidemic dynamics. As stated above, we postulate a model that explicitly links epidemiological and immunological dynamics through an inoculation term that depends on the abundance of infected mosquitoes. This approach, is based on separating biological time scales: a fast time scale associated with the within-host dynamics and a slow time scale associated with the epidemiological process. One of the advantages of this approach is that an explicit linkage between the two processes is established through infected mosquitoes: within our approach, a bite from an infected mosquito inoculates an extra viral load into the host that connects, the population dynamics with the within-host dynamics of the disease. At the same time, an infected mosquito transmits the pathogen to the vertebrate host with an intensity or level that depends on the viral load or the level of cell infection within the host.

The paper is organized as follows: Section 2 presents the mathematical model and an endemic scenario; in Section 3, we discuss the conditions for a disease outbreak; and finally, in Section 4, we present our conclusions.

2. Mathematical model

The dynamics of the Ross-Macdonald model represent the archetypal example of a vector-borne endemic disease. If the reproductive number is greater than one, then an asymptotically stable endemic state exists and the disease-free equilibrium is unstable. If the reproductive number is below one, then the disease-free state is the only equilibrium. In this section, we look at an endemic infectious disease that is vector-borne. Thus, we couple the classical Ross-Macdonald model for a vector-host

system with the standard within-host model. We think of our hosts as a general vertebrate species, while the vector is generally a mosquito. In the epidemiological model, I represents the number of infected vertebrate individuals, and Y represents the number of infected mosquitoes. The variables T and T^* correspond to the immunological dynamics and represent uninfected and infected target cells, respectively. v represents the virus concentration in the plasma of an average infected vertebrate host. μ and δ represent mortality rates for the vertebrate host and mosquito, respectively and γ is the recovery rate of the vertebrate hosts. The parameters $\alpha = \alpha(x)$ and $\beta = \beta(x')$ represent the effective contact rates from mosquito to animal and from animal to mosquitoes, respectively and are assumed to depend, in general, on some measure of infectiveness either in the mosquito, denoted by x, or the vertebrate host, x'. The most common assumption for these functions [22, 23] is that they satisfy $\alpha(x), \beta(x') \geq 0$, $\alpha'(x), \beta'(x') > 0$, and $\alpha''(x), \beta''(x') \leq 0$ for $x, x' \in [0, \infty)$. In our model, $\beta(x')$ is the biting rate that transmits the disease from an infected host with an infectiousness of x' to a susceptible mosquito. Our model assumes that the biting rate from the infected mosquito to a susceptible host, $\alpha(x)$, will be proportional to $\beta(x')$. Some evidence which supports this hypothesis is in the work of Tesla et al. [14], who reported that increasing the viral dose for Zika in the blood meal increases the probability of mosquitoes becoming infected and becoming infectious. In this sense, additional findings which support this hypothesis can be found in previous experimental and modeling studies [24,25]. In summary, the rationale of this assumption is that a high viral load in the vertebrate host will generate a high viral load infection in the mosquito, which will induce an infectious effective biting rate. Effectively, $\alpha(x)$ represents the effective contact rates from the mosquito to the vertebrate host. Since we are not following the within-mosquito dynamics, we will let α be a free parameter; likewise, $\beta(x') = a\phi(x')$, where $\phi(x')$ is the probability of mosquito infection per bite. The equations for the between-host system are a variant of the so-called Ross-Macdonald equations:

$$\begin{aligned} I' &= \alpha(x)\Big(\frac{N-I}{N}\Big)Y - (\mu+\gamma)I, \\ Y' &= \beta(x')(M-Y)\frac{I}{N} - \delta Y, \end{aligned} \tag{2.1}$$

where N and M are the total constant populations of the vertebrate hosts and mosquitoes, respectively. Normalizing Eq (2.1) by defining $i = I/N$, $y = Y/M$, and $q = M/N$, we can rewrite them as follows:

$$\begin{aligned} i' &= \alpha(x)q(1-i)y - (\mu+\gamma)i, \\ y' &= \beta(x')(1-y)i - \delta y, \end{aligned} \tag{2.2}$$

For the within-host system, T, T^*, and V represent the target cells, infected target cells, and virions, respectively; as for the parameters, λ represents the recruitment rate of the healthy target cells, m the natural mortality rate of the target cells, k the cell-infection rate, d the virus-induced cell death, p the virus proliferation rate per infected cell, c the viral clearance rate, and $g = g(y)$ is an inoculation term that depends on the abundance of infected mosquitoes. The equations for the within-host dynamics are as follows

$$\begin{aligned} T' &= \lambda - kVT - mT, \\ T^{*'} &= kVT - dT^*, \\ V' &= pT^* - cV + g(y). \end{aligned} \tag{2.3}$$

The model is a coupled system given by Eqs (2.2) and (2.3). The variable and parameter meanings are given in Table 1.

Table 1. Definition of variables and parameters for systems (2.2) and (2.3).

Notation	Description
Between-host model	
i	Population of infectious vertebrate hosts.
y	Population of infectious mosquitoes.
$\alpha(x)$	Effective contact rates from mosquito to host.
$\beta(x')$	Effective contact rates from host to mosquito.
q	Ratio of mosquitoes and hosts.
γ	Recovery rate of vertebrate hosts.
δ	Vector mortality rate.
μ	Host mortality rate.
Within-host model	
T	Target cells.
T^*	Infected target cells.
V	Virions.
λ	Cell recruitment rate.
k	Cell infection rate.
m	Naive cell mortality rate.
d	Infected cell mortality rate.
p	Viral production rate.
c	Viral clearance rate.
$g(y)$	Inoculation term as a function of infected mosquitoes.

An epidemiological model is studied below. The virus concentration in the plasma of an average infected vertebrate host increases due to the feedback from the population-level infection (i.e., infected mosquitoes). This process is incorporated in the feedback function, $g(y)$, where y gives the number of infectious mosquitoes $y > 0$. To link the abundance of infected mosquitoes with the infection process at the individual level, we assume that the infected mosquitoes directly correlate with the level of infected target cells. This biological consideration suggests that the function g should have the following properties: $g(y) > 0$, $g(0) = 0$, $g'(y) > 0$, and $g''(y) \leq 0$. Thus, in the absence of the feedback ($y = 0$), when the virus is independent of the population-level infection, the virus within the host reaches the steady state value. We performed the analysis using numerical simulations for the case when $g(y) > 0$.

In general, as in [2, 4], several functional forms can be considered for $g(y)$, and we take $g(y) = ry^s$ with $r, s > 0$. In the next section, we restrict our analysis to the case $s = 1$ as we aim to illustrate the framework of linking the within- and between-host dynamics for viral load-dependent contact rates.

The model described in [1–3], is a conceptual model for the dynamics of *Toxoplasma gondii*, in which the life cycle of the parasite includes interactions with the environment. Unlike vector-borne diseases, these are not environmentally transmissible; therefore, the inclusion of the inoculation rate

$g(y)$ is key to link the within-host dynamics to the between-host dynamics as a feedback function for v dynamics.

2.1. Biting rates dependent upon within-host states

An essential biological feature of this coupled system is that the within-host dynamics occur on a faster time scale than the dynamics of the between-host and the environment. Multiple time scales allow us to study the mathematical properties of the model by separately analyzing the fast- and slow systems determined by the two time scales. As evidence that supports this analysis, we can cite [26], which reported on the duration of DEN-1 viremia in a clinical study. Here, the duration of viremia ranged from 1 to 7 days (mean, 4.5 days; median, 5 days), with viremias of the primary infection lasting more compared to the secondary infections: the mean duration of viremia for all patients who experienced a primary dengue virus infection was 5.1 days versus 4.4 days for those with a secondary dengue virus infection. In contrast, dengue outbreaks last several months, or, in endemic situations, transmission takes place over the years, as reported in [27] or the statistics provided by the Pan American Health Organization (PAHO) [28], among many other sources.

By [1–3], our objective is to distinguish between the slow and fast subsystems that belong to either the between-host (epidemiological) or the within-host (immunological) models. For the fast subsystem [2, 3], we only utilize the outcomes directly relevant to our objective and refer the reader to the mentioned reference for additional information. The within-host dynamics (2.3) can be considered a fast system where the variable y can be treated as a constant (i.e., it is not changing with time on the fast time scale). In our case (Eq (2.3)), when $g(y) = 0$, the system always has the infection-free equilibrium $E_0 = \left(T_0, T_0^*, V_0\right)$, where $T_0 = \frac{\lambda}{m}$, $T_0^* = 0$, $V_0 = 0$, and there are no virions or infected cells. Let $R_v(y)$ denote the within-host reproduction function that depends on the mosquito density; then, define $R_{0v} = R_v(0)$ given by the standard formula for the within-host model

$$R_{0v} = \frac{\lambda k p}{m c d}$$

as the basic reproduction number of the uncoupled fast (within-host) system.

Let $x' = T^*(t)/T_0$, which represents the proportion of infected target cells at time t, and is a measure of the infectiousness of the vertebrate host. Let

$$\beta(x') = a\phi(x'), \qquad \phi(x') = (x')^z$$

with $z > 0$ and $a > 0$, the biting rate. In the case of vertebrate infections, these depend on the infectiousness of the mosquito bite. Then, the between-host basic reproduction number is as follows:

$$R_b(x') = \sqrt{\frac{a^2 b q \phi(x')}{(\gamma + \mu)\delta}}. \tag{2.4}$$

Note that if $x' = 1$, then

$$R_b(1) = \sqrt{\frac{a^2 b q \phi(1)}{(\gamma + \mu)\delta}},$$

is the maximum biologically feasible reproduction number as a function of the host infectiousness x'. When $R_b(x') > 1$, the (between-host) endemic equilibrium point can exist and is explicitly given as follows:

$$i^* = \frac{\delta(\gamma+\mu)(R_b^2(x')-1)}{a\phi(x')(qab+\gamma+\mu)}, \qquad y^* = \frac{\delta(\gamma+\mu)(R_b^2(x')-1)}{qab(a\phi(x')+\delta)}.$$

Both of these coordinates depend on x' and will render the between-host endemic equilibrium when $x'_* = \hat{T}^*/T_0$; the equilibrium between the infected target cell and infection with the nontrivial equilibrium $(\hat{T}(y), \hat{T}^*(y), \hat{V}(y))$ is as follows:

$$\hat{T}^*(y) = \frac{m}{d}\left(T_0 - \hat{T}(y)\right), \qquad \hat{V}(y) = \frac{1}{c}\left(g(y) + p\hat{T}^*(y)\right). \tag{2.5}$$

$$\hat{T}(y) = \frac{1}{2}\left(a_1 - \sqrt{a_1^2 - 4a_2}\right) \tag{2.6}$$

with

$$a_1 = \frac{g(y)d}{pm} + T_0\left(1 + \frac{1}{R_{0v}}\right), \qquad a_2 = \frac{T_0^2}{R_{0v}}. \tag{2.7}$$

An alternative way of looking at the between-host endemic equilibrium is as follows. The endemic equilibrium point (slow subsystem) (i^*, y^*) is located at the intersection of the zero isoclines of the between-host equations (for constant within-host dynamics). These are as follows:

$$y = \frac{a\phi(x')i}{a\phi(x')i + \delta}, \qquad y = \frac{abi(\gamma+\mu)}{q(1-i)}. \tag{2.8}$$

The intersection exists with a positive i whenever $R_b(x') > 1$, which we call the *basic reproduction function*. However, in this case, our equilibrium is located on the line that describes this intersection as a function of the parameter x' (see Figure 1). Still, the value of the basic reproduction number R_{0b} will only be determined when $x' = x'_*$, which implies that $R_b(x'^*) = R_{0b} \leq R_b(1)$ (i.e., the maximum of the between-host reproduction function bounds the between-host basic reproduction number). On the other hand, the dependence of the quantity $x' = T^*/T_0$ on c is linear. The within-host reproductive number is a decreasing function of c [1].

In consequence, given c such that $R_{0v} > 1$, as the clearance rate increases (the viral life cycle is faster), the proportion of infected target cells decreases; however, the approach to the equilibrium becomes slower as c increases (see Figure 2a) because, at the same time, the within-host reproduction number R_{0v} decreases and approaches 1. As c further increases, there is a value c^* such that if $c > c^*$, then the non-trivial within-host equilibrium is no longer feasible, which implies that the within-host infection is not sustained, thus bringing to extinction the epidemic. This is due to the reduction of R_{0v}, which weakens the ability of the virus to sustain an infection within the host. At the same time, the transient period before reaching an equilibrium becomes longer as R_{0v} approaches the critical threshold. When c exceeds a certain value c^*, the non-trivial equilibrium is no longer feasible and the infection dies out. While these results directly arise from the mathematical structure of the model, we recognize that their biological validity depends on the applicability of the assumptions and parameter values used, and should not be interpreted as universally generalizable findings.

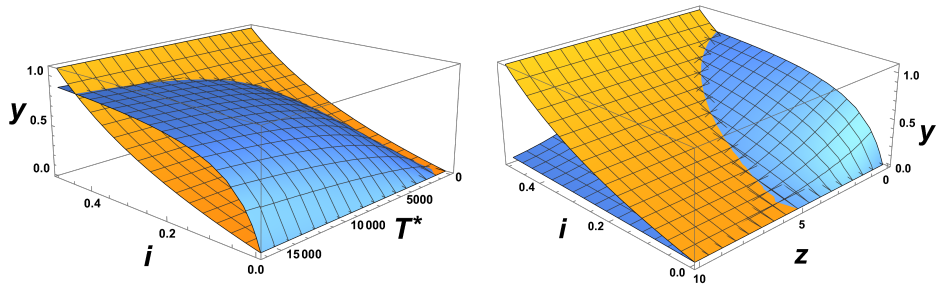

(a) 3D representation of the zero-isoclines (Eq (8)) for the between-host model as a function of T^*, the infected target cells. x-axis is i, y-axis is T^* with $z = 0.8$. The blue-shaded region describes the transcritical bifurcation that appears. The endemic equilibrium point occurs when T^* reaches the critical value such that $R_b(x') = 1$. Parameters: a=1, $b = 1$, $\delta = 1/15$, $z = 0.8$, $q = 5$, $\mu = 1/(70) * 635$, $\gamma = 1/7$, $\lambda = 5000$, $m = 0.31$, $R_b(x') > 1$.

(b) 3D representation of the zero-isoclines (Eq (8)) for the between-host model as a function of z, the exponent of the mosquito biting rate. x-axis is i, y-axis is z. The blue-shaded region describes the transcritical bifurcation region that appears. The endemic equilibrium point occurs when T^* reaches the critical value such that $R_b(x') = 1$. Parameters: a=1, $b = 1$, $\delta = 1/15$, $T^* = 10,000$, $q = 5$, $\mu = 1/(70)*635$, $\gamma = 1/7$, $\lambda = 5000$, $m = 0.31$, $R_b(x') > 1$.

Figure 1. Isoclines of the between-host system as functions of model parameters.

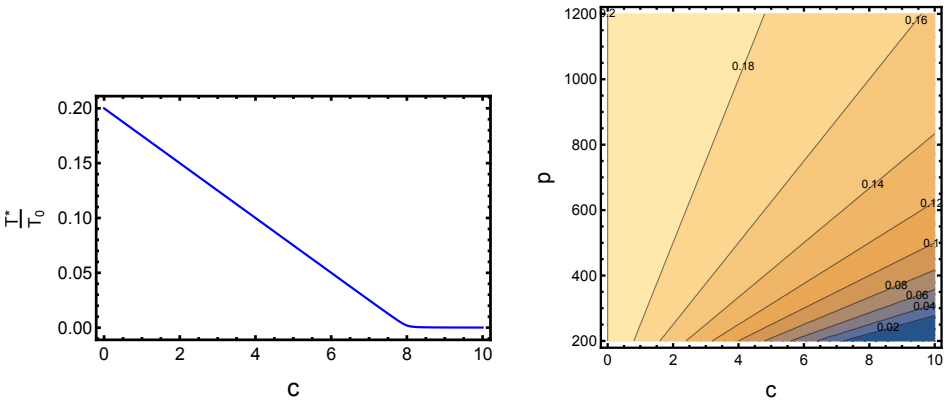

(a) Proportion of infected host cells T^*/T_0 as a function of the clearance rate c (Eq (2.6)). Beyond $c = 8$ the within-host non-trivial equilibrium ceases to exist and the disease-free equilibrium is the only attractor.

(b) Contour plot of T^*/T_0 as a function of c, the clearance viral rate horizontal axis, and p, the viral production rate vertical axis.

Figure 2. Dependence of the proportion of infected target cells T^*/T_0 (Eq (2.6)) on the viral production and clearance rates.

On the other hand, if c is small, then the equilibrium quantity T^*/T_0 is very close to 1, and the within-host reproductive number is large, which implies an active within-host infection and a positive prevalence at the epidemic level (see Figure 3). The formulation of the coupled model involves the feedback from the infected vector to the within-host level via the function $g(y)$. Given this feature of the model, implementing the fast and slow framework requires that the death rate of the infected cells be greater than the natural death rate in mosquitoes (i.e., $d > \delta$) for the feedback from infected

mosquitoes into the within-host dynamics; likewise, from the infected hosts into the within-host level, (i.e., $d > \gamma$). These fast-slow assumptions are satisfied by the baseline parameter values utilized in Table 2.

We have seen that the effect of the within-host dynamics on the between-host subsystem basically resides in the time it takes for the virus load or number of infected target cells to reach the appropriate level such that R_{0b} is reached; then, an epidemic outbreak will take place. Once this threshold is reached, the between-host system dynamics is essentially that of the classical Ross-Macdonald model.

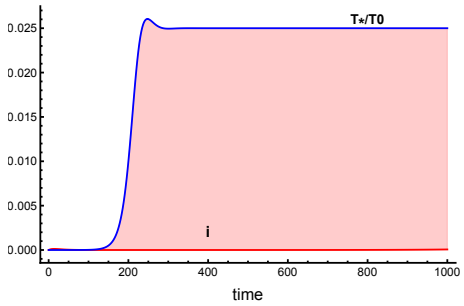

(a) Behavior of T^*/T_0 (blue line) for large c (fast clearance rate), in this case $c = 7$. The threshold at which $R_{0w} = 1$ is $c^* = 8$. For c above this threshold, the WH equilibrium does not exist. Red line i, host infection level (increasing but imperceptible in this scale). Note the long delay for the epidemic to take off compared to b).

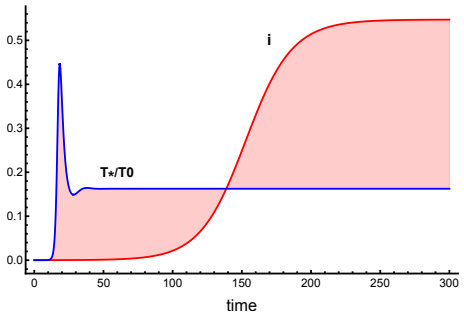

(b) Behavior of T^*/T_0 (blue line) for small c (slow clearance rate), in this case $c = 1.5$. The threshold at which $T^*/T_0 = 1$ is $c = 1.1$. For c below this threshold, the equilibrium is unfeasible. Red line i, host infection level.

Figure 3. Behavior of the between- and within-host systems as a function of c. The blue line is the number of infected target cells T^*; the red line is the host prevalence. Parameter values as in Table 2 except for c.

Table 2. Baseline parameter values for the figures shown. Data from [29].

Parameter	Definition	Value	Units
α	effective contact rate	free parameter	[1/vector ×d]
z	scaling	1/2	dimensionless
q	ratio of mosquitoes and hosts	1.5	dimensionless
γ	recovery rate	1/10	[1/d]
μ	host mortality rate	1/(365)(70)	[1/d]
δ	vector mortality rate	1/20	[1/d]
k	cell infection rate	2×10^{-7}	[1/virion×d]
p	viral production rate	200	[virions]
c	viral clearance rate	5	[1/d]
λ	cell recruitment rate	10,000	[cell/d]
m	naive cell mortality	1/10	[1/d]
d	infected cell mortality	0.5	[1/d]
r	vector viral influx	0	[virion/vector×d]

Therefore, the result illustrated in Figure 2 is, contrary to the results on dengue reported by [30],

where short viremias have larger viral loads than long viremias. Due to the way the within-host dynamics is modeled and the resulting form that the within-host reproduction number takes, a large c (short viremias) reduces the magnitude of the reproductive number and, therefore, generates lower viremias than when c is small (long viremias). For dengue disease, [30] used a more detailed model which is carefully adapted to dengue viral dynamics that is able to capture dynamical characteristics that our simple model cannot achieve. Our simple model does not consider any specific activation mechanisms of innate and adaptive immune responses. Thus, our results cannot be directly compared to those in [30]. However, the results on malaria [31] may seem to agree with the relation of clearance and pathogen load that our model produces; however, this similarity is only anecdotal since malaria is a parasitic disease, where the parasites have specific, and sometimes different, life stages in the host [32]. In this work, it is clear that the length of the pathogen clearance time is associated with higher concentrations of parasites. For Zika, [33] reported relatively long viremias in the whole blood samples of human hosts of more than 26 days, while in macaques [34], the highest viremia was reported for intermediate duration (in macaques the viremia length ranges from 2 to 7 days); for Chikungunya, [35], the higher frequency of high viremia in the human hosts also occurred on the 7th day of symptom onset (symptom onset occurs in the interval 1–20 in this study). As we discussed in the text, the between-host reproduction number will be greater than one until enough infection has accumulated to sufficiently increase the ratio $x' = T^*(t)m/\lambda$. When the between-host reproduction number that depends on x' is less than one, the only equilibrium point is the disease-free equilibrium, which is asymptotically stable.

3. Conditions for a disease outbreak

In our model, we assume that the host's internal state influences the rates of disease transmission and the virulence of the disease. According to [8], the infectiousness of a host will grow with the viral load, and the host's survival rate will drop as the infection takes over more resources (such as the target cells that are the target of the infection). Therefore, we propose that in the between-host model, the parameters β and γ, can be written as functions of the proportion of infected target cells x'. To keep things simple, we disregard the within-host model's transitory dynamics and assume that the within-host system is consistently in equilibrium during the infection, or equivalently to assume that the within-host dynamics is fast compared to those of transmission and host mortality.

From the perspective of natural selection acting within a host, the optimal clearance rate of the pathogen c^* implies an active within-host infection; as the equilibrium state of the within-host system is a function of the rate clearance rate, it follows that β and γ can be written as functions of c (see, [8]).

According to the above statement, the existence of an epidemic outbreak depends on the strength of the infection at the within-host level measured by the within-host reproduction number when $R_{0v} > 1$. When $0 < R_b(x') < 1$, the only between-host equilibrium point is the disease-free equilibrium, which is asymptotically stable. $R_b(x') > 1$ requires the average individual in the population to have an active (within-host) viral infection. Still, the transmission efficacy will not be large enough to trigger an epidemic until $R_b(x') = R_{0b}$. We can give a more detailed description of the dependence of the between-host equilibrium state and the within-host dynamics. First, there exists a critical value of $T^* = \hat{T}_*$ where $R_b(\hat{T}^*) = 1$. In Figure 1a, we plot the intersection of Eq (2.8) to show how the existence of an endemic equilibrium depends on T^* and i. As T^* increases above $\hat{T}^*$, the boundary between the two colored regions shown in the figure is the line containing the feasible endemic equilibrium realized when T^*

reaches its steady state. A second important feature is associated with the contact rate $\beta(x') = a\phi(x')$, where $\phi(x') = (x')^z$. Figure 1b shows the intersection of the two isoclines Eq (2.8) that give the feasible endemic equilibrium but as functions of x' and z, the exponent of the probability of infection $\phi(x')$. Large values of z prevent an endemic between-host equilibrium point, whereas, for $z \leq 1$, the endemic equilibrium always exists. Additionally, the endemic level is higher when $z < 1$. Therefore, concave infection probabilities always generate an endemic state, provided $R_{b0} > 1$, while convex ones do not. A third observation is that we can expect a variable-duration time delay between crossing the threshold $R_b(T*) = 1$ and the time when the epidemic outbreak occurs and sends the between-host system to its endemic state (i.e., when $R_b(T*) = R_0$). This delay appears because our contact rate parameters, which depend on within-host dynamics, are dynamic.

3.1. The coupled system: endemic scenario

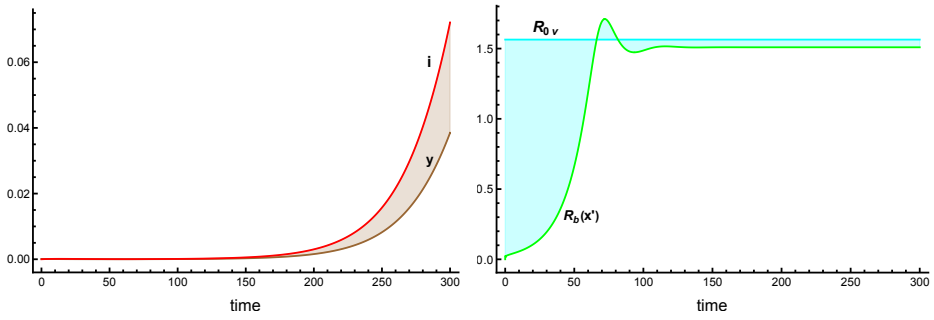

(a) Growth of the infected hosts i (red) and infected vectors y (brown) at the initiation of the epidemic outbreak.

(b) Within-host reproduction number R_{0v} (cyan) and between-host reproduction function $R_b(x')$ given by Eq (2.4) (green).

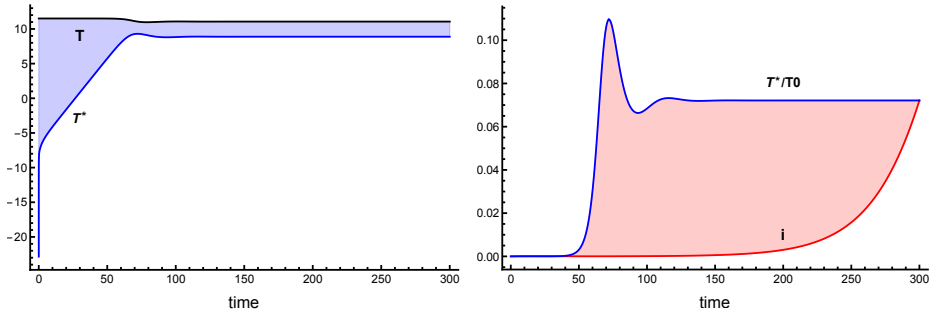

(c) Naive target cells T (black) and infected target cells T^* (blue). Logarithmic scale.

(d) Infected hosts i (red) and the ratio infected target cells to the initial number of target cells $T^*(t)/T_0$ (blue). Note the difference in the temporal scale of both processes. $c = 5.115$.

Figure 4. Basic dynamics of systems given by Eqs (2.3) and (2.2) for the baseline parameter values described in Table 2.

Now, we look at the role of virulence, measured by our variable x', on the dynamics of our system. First, we make the reasonable assumption that the recovery rate γ is not constant but satisfies the following:

$$\gamma(x') = \gamma(1 - x'),$$

which implies that a large virulence is associated with chronic disease with practically no recovery, and low virulence makes the recovery rate $\gamma(x')$ approximately equal to the baseline γ. Recall $R_b(x')$ given by Eq (2.4). On the other hand, the endemic equilibrium for the host population, has the following formula

$$i^* = \frac{\delta(\gamma(1-x')+\mu)x'^{-z}}{a(abq+\gamma(1-x')+\mu)}(R_b^2(x')-1). \tag{3.1}$$

The within-host and between-host population processes are closely coupled, as can be seen in the timing at which an equilibrium is reached for both subsystems. In Figure 4, we show typical trajectories for the baseline values.

The observed delay in the onset of the epidemic (see Figure 4a) at the between-host level is associated with the particular shape of the probability of infection $\phi(x') = (x')^z$ (see Eq (6)) from mosquito to host; therefore, the ratio of mosquito numbers to host numbers is associated with the speed at which the within-host subsystem increases the proportion of infected cells (Figure 4c,d). Figure 4(b) shows the relative magnitude of the within-host (constant) reproduction number and the between-host reproduction function as x' changes.

However, the between-host reproduction function approaches its limit $R_b(T^*)$ at different speeds depending on the magnitude of z. The epidemic outbreak will be triggered when the within-host system reaches an equilibrium, regardless of how significant the within-host infection is while approaching it. Therefore, our model indicates that transmission at the population level is feasible but cannot be realized until the average infection conditions of individuals reach their corresponding equilibrium. Therefore, the reproduction number of the between-host system indicates an epidemic outbreak that will occur later, depending upon the magnitude of T^*. This is one of the explicit links between the population-level reproduction number and the within-host infection dynamics. Figures 5a,b show the system dynamics observed when the within-host reproduction number is $R_{0v} > 1$. Still, there is no significant epidemic outbreak even when the viral influx from the inoculum is relatively large. In this case, the between-host reproduction function cannot exceed the threshold $R_{0b} = 1$ because the level of cell infection remains relatively low, and the mosquito biting rate linearly increases with the viral load. This linear relationship limits the efficiency of transmission compared to scenarios where the biting rate accelerates. The between-host reproduction function is asymptotic to $R_{0b} < 1$. Figure 5c,d illustrate the behavior of the system when the within-host reproduction number is $R_{0w} < 1$. In this case, the epidemic outbreak is suppressed even when the viral influx from inoculation is large ($r = 10,000$). In this case, the between-host reproduction function is also asymptotic to $R_{0b} < 1$ but much lower than in Figure 5b. Finally, Figure 6 shows the endemic equilibrium i^* (Eq (3.1)) as a function of the baseline host recovery rate γ (we have that the effective recovery rate is $\gamma(1-x')$ form the baseline due to our hypothesis that the recovery rate depends on the proportion of infected cells).

Notice that for a given prevalence, the infection level required to reach it is relatively small when the recovery time is fast (order of days, small γ) and large (recovery period on the order of weeks or longer) otherwise.

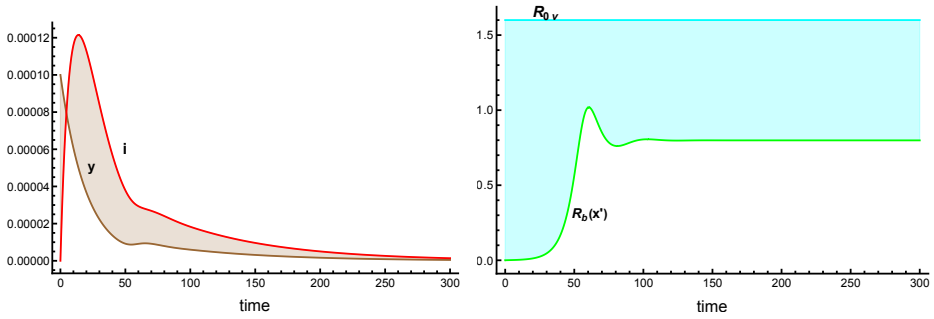

(a) Growth of the infected hosts i (red) and infected vectors y (brown) for the scaling parameter $z = 1$, $p = 100$ and the viral influx rate $r = 10,000$.

(b) Within-host reproduction number R_{0v} (cyan) and between-host reproduction function $R_b(x')$ given by Eq (2.4) (green) for the parameter values described in a). $R_{0w} > 1$ and $R_{0b} < 1$. Parameters: $z = 1$, $p = 200$, $c = 5$, $r = 10,000$.

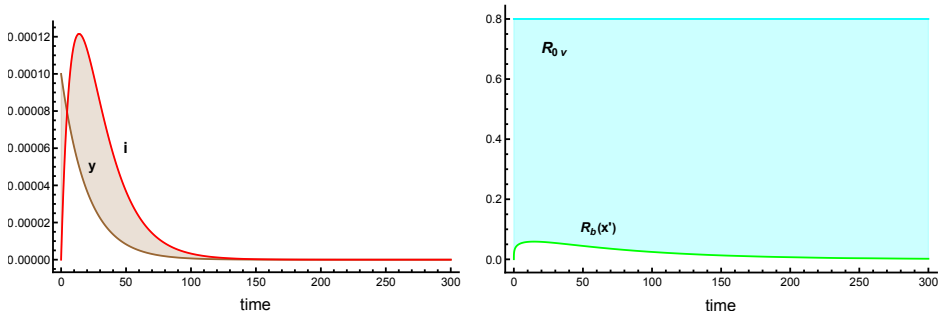

(c) Growth of the infected hosts i (red) and infected vectors y (brown) for the scaling parameter at its baseline value $z = 1$ but $p = 100$. The viral influx rate is $r = 10,000$.

(d) Within-host reproduction number R_{0v} (cyan) and between-host reproduction function $R_b(x')$ given by Eq (2.4) (green) for the parameter values described in c). $R_{0w} < 1$ and $R_{0b} < 1$ but much lower than in b). Parameters: $z = 0.5$, $p = 100$, $c = 5$, $r = 10,000$.

Figure 5. Basic dynamics of systems given by Eqs (2.3) and (2.2) for changes in the scaling parameter and the influx of viral particles due to the term ry in Eq (2.3).

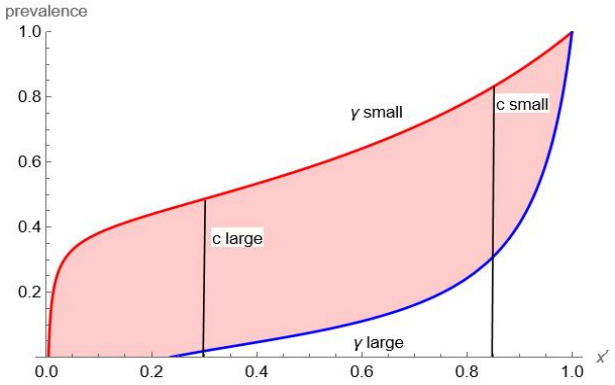

Figure 6. Host prevalence as a function of x', the average proportion of infected cells in the host. The curves plot Eq (3.1) for large (blue) or small (red) values of the recovery rate γ. All other parameters as in Table 2.

4. Conclusions

In this study, we developed and analyzed a model that explicitly integrates the interaction between epidemiological dynamics at the population level and immune-virus dynamics within the host. Unlike many existing models that treat these two processes as separate and largely independent, our approach provides a direct and coherent linkage between them. By doing so, we aimed to capture essential biological mechanisms which govern the spread and persistence of vector-borne diseases while also incorporating the host's immunological response to infection. Our model is based on two well-established frameworks: the Ross-Macdonald model for vector-borne disease transmission and a basic virus-cell interaction model that describes the within-host viral dynamics. The combination of these classical approaches allows us to explore the fundamental principles which govern the interplay between host immunity, viral replication, and disease transmission dynamics.

There are fundamental differences between environmental transmission (in our model $g(y)$) and vector-borne transmission, particularly the distinction between passive and active modes of pathogen transmission. This distinction is indeed a key factor in determining the appropriate modeling strategies. The biological interpretation changes (i.e., the biological mechanisms differ), so our justification for modeling vectors as an environmental stage lies in the mathematical tractability of separating time scales and incorporating an intermediate transmission stage. By focusing on the transmission dynamics and the resulting epidemiological consequences, we are able to capture key aspects of the within-host and between-host interaction.

In our model, the proportion of infected target cells decreased as a function of the viral clearance rate c, which was independent of the asymptotic level of infection or prevalence in the vector population (Figure 2a). However, the clearance rate of the virus plays a critical role in shaping both the within-host and the between-host dynamics. Specifically, a faster clearance rate extends the transient period before the system reaches equilibrium, thus delaying the onset of an epidemic at the population level (Figure 3a). In contrast, a slower clearance rate leads to a higher within-host reproduction number, thereby accelerating the infection of target cells and shortening the time required for a between-host outbreak to emerge. Another parameter of importance is the viral production rate p. In our model, increased the viral production rate increases R_{0v}; as p increased, the sensitivity of T^*/T_0 to the magnitude of the clearance rate c significantly decreased (Figure 2b). As shown in [1], in this within-host model, fast clearance rates represent low viral loads. Thus, a low T^* and slow clearance rates are associated with high viremias, and therefore high proportions of infected cells.

Another observation is that the inoculation rate $g(y)$ has a marginal role in the dynamics of the outbreak. This finding arises under the specific assumptions and structure of the model. In particular, when the within-host reproduction number R_{0v} is low or the host recovery is rapid, the host environment may not sustain viral replication over time, which reduces the long-term impact of the inoculum. However, we acknowledge that in biological systems, especially during early outbreak stages or under stochastic conditions, the pathogen introduction rate can be a critical determinant of the transmission success. Thus, the marginal effect of inoculation observed here should be interpreted as a theoretical consequence of the model's structure, rather than a generalizable prediction.

Additionally, our results illustrate that the epidemic potential of the disease critically depends on the recovery time of the infected individuals. Specifically, the viral clearance rate c determines whether an epidemic can sustain itself. When the recovery times are relatively short (i.e., the immune system clears

the virus quickly), the viral generation time is too short to support an active outbreak, as indicated by the condition $R_{0b} < 1$. In contrast, for infections with long recovery times (small γ), the basic reproduction number R_{0b} rapidly exceeds the epidemic threshold, thus allowing disease outbreaks even when the average infection levels are low.

From a broader perspective, our model illustrates that, under its assumptions, diseases characterized by long viral generation times (small c) may exhibit a higher prevalence, particularly when the recovery period is also prolonged. Although the model was not calibrated to specific pathogens, we used the contrasting clinical profiles of dengue fever and West Nile virus to illustrate this concept. Dengue typically has a short recovery time (usually less than a week), whereas West Nile virus infections can persist for several months in some hosts [36]. These differences in recovery dynamics, while not directly modeled here, highlight the potential relevance of the within-host persistence in shaping the transmission potential and epidemic duration. Our findings suggest that such persistence could contribute to sustained transmission chains, even when the observed prevalence of active cases remains relatively low.

While our model adopted a general and simplified framework based on classical formulations of the within-host and between-host dynamics, the conclusions drawn must be interpreted with care. The patterns we identified such as the influence of the viral clearance rate, recovery time, and viral production on transmission potential are not universally applicable, but rather illustrate how specific mechanisms may interact under the assumptions of our model. The value of this approach lies not in its ability to provide predictive outcomes for particular diseases, but in highlighting potential trade-offs and interdependencies between immunological and epidemiological processes that may be relevant across a range of vector-borne infections.

In this sense, we emphasize that our goal is not to quantitatively model a specific vector disease. Instead, we presented a conceptual framework that explored how the within-host factors such as viral replication and immune clearance can shape the conditions for population-level transmission. The insights provided here should be viewed as theoretical contributions derived from a deterministic system under idealized assumptions. Further work, including empirical parameterization and pathogen-specific dynamics, will be essential to translate these ideas into concrete epidemiological predictions.

Use of AI tools declaration

The authors declare they have not used Artificial Intelligence (AI) tools in the creation of this article.

Acknowledgments

JACE and JXVH acknowledge support from UNAM through grant PAPIIT IV100220. MNL acknowledges the financial support from the Asociación Mexicana de Cultura, A.C.

Conflict of interest

The authors declare there is no conflict of interest.

References

1. Z. Feng, J. X. Velasco-Hernández, B. Tapia-Santos, A mathematical model for coupling within-host and between-host dynamics in an environmentally-driven infectious disease, *Math. Biosci.*, **241** (2013), 49–55. https://doi.org/10.1016/j.mbs.2012.09.004
2. Z. Feng, J. X. Velasco-Hernández, B. Tapia-Santos, M. Leite, A model for coupling within-host and between-host dynamics in an infectious disease, *Nonlinear Dyn.*, **68** (2012), 401–411. https://doi.org/10.1007/s11071-011-0291-0
3. Z. Feng, X. Cen, Y. Zhao, J. X. Velasco-Hernández, Coupled within-host and between-host dynamics and evolution of virulence, *Math. Biosci.*, **270** (2015), 204–212. https://doi.org/10.1016/j.mbs.2015.02.012
4. X. Cen, Z. Feng, Y. Zhao, Emerging disease dynamics in a model coupling withinhost and between-host systems, *J. Theor. Biol.*, **361** (2014), 141–151. https://doi.org/10.1016/j.jtbi.2014.07.030
5. M. A. Gilchrist, A. Sasaki, Modeling host-parasite coevolution: A nested approach based on mechanistic models, *J. Theor. Biol.*, **218** (2002), 289–308. https://doi.org/10.1006/jtbi.2002.3076
6. A. E. S. Almocera, V. K. Nguyen, E. A. Hernández-Vargas, Multiscale model within-host and between-host for viral infectious diseases, *J. Math. Biol.*, **77** (2018), 1432–1416. https://doi.org/10.1007/s00285-018-1241-y
7. N. Mideo, S. Alizon, T. Day, Linking within- and between-host dynamics in the evolutionary epidemiology of infectious diseases, *Trends Ecol. Evol.*, **23** (2008), 511–517. https://doi.org/10.1016/j.tree.2008.05.009
8. M. Gilchrist, D. Coombs, Evolution of virulence: interdependence, constraints, and selection using nested models, *Theor. Popul. Biol.*, **69** (2006), 145–153. https://doi.org/10.1016/j.tpb.2005.07.002
9. F. Saldaña, J. X. Velasco-Hernández, Modeling the COVID-19 pandemic: a primer and overview of mathematical epidemiology, *SeMA J.*, **79** (2022), 225–251. https://doi.org/10.1007/s40324-021-00260-3
10. H. Gulbudak, V. L. Cannataro, N. Tuncer, M. Martcheva, Vector-borne pathogen and host evolution in a structured immuno-epidemiological system, *Bull. Math. Biol.*, **79** (2017), 325–355. https://doi.org/10.1007/s11538-016-0239-0
11. M. Martcheva, N. Tuncer, Y. Kim, On the principle of host evolution in host–pathogen interactions, *J. Biol. Dyn.*, **11** (2017), 102–119. https://doi.org/10.1080/17513758.2016.1161089
12. H. Gulbudak, An immuno-epidemiological vector-host model with within-vector viral kinetics, *J. Biol. Syst.*, **28** (2020), 233–275. https://doi.org/10.1142/S0218339020400021
13. R. M. Ribeiro, A. S. Perelson, The analysis of HIV dynamics using mathematical models, in *AIDS and Other Manifestations of HIV Infection*, **905** (2004), 912.
14. B. Tesla, L. R. Demakovsky, H. S. Packiam, E. A. Mordecai, A. D. Rodríguez, M. H. Bonds, et al., Estimating the effects of variation in viremia on mosquito susceptibility, infectiousness, and R0 of Zika in Aedes aegypti, *PLoS Negl. Trop. Dis.*, **12** (2018). https://doi.org/10.1371/journal.pntd.0006733

15. B. W. Alto, K. Wiggins, B. Eastmond, D. Velez, L. P. Lounibos, C. C. Lord, Transmission risk of two chikungunya lineages by invasive mosquito vectors from Florida and the Dominican Republic, *PLoS Negl. Trop. Dis.*, **11** (2017), e0005724. https://doi.org/10.1371/journal.pntd.0005724

16. L. Lambrechts, R. C. Reiner, M. V. Briesemeister, P. Barrera, K. C. Long, W. H. Elson, et al., Direct mosquito feedings on dengue-2 virus-infected people reveal dynamics of human infectiousness, *PLoS Negl. Trop. Dis.*, **17** (2023), e0011593. https://doi.org/10.1371/journal. pntd.0011593

17. S. M. Lemon, P. F. Sparling, M. A. Hamburg, D. A. Relman, E. R. Choffnes, A. Mack, *Vector-Borne Diseases: Understanding the Environmental, Human Health, and Ecological Connections: Workshop Summary*, The National Academies Press, 2008. https://doi.org/10.17226/11950

18. N. L. González Morales, M. Núñez-López, J. Ramos-Castañeda, J. X. Velasco-Hernández, Transmission dynamics of two dengue serotypes with vaccination scenarios, *Math. Biosci.*, **287** (2017), 54–71. https://doi.org/10.1016/j.mbs.2016.10.001

19. S. Bhatt, P. W. Gething, O. J. Brady, J. P. Messina, A. W. Farlow, C. L. Moyes, et al., The global distribution and burden of dengue, *Nature*, **496** (2013), 504–507. https://doi.org/10.1038/nature12060

20. C. A. Hill, F. C. Kafatos, S. K. Stansfield, F. H. Collins, Arthropod-borne diseases: vector control in the genomics era, *Nat. Rev. Microbiol.*, **3** (2005), 262–268. https://doi.org/10.1038/nrmicro1101

21. F. Beugnet, M. Jean-Lou, Emerging arthropod-borne diseases of companion animals in Europe, *Vet. Parasitol.*, **163** (2009), 298–305. https://doi.org/10.1016/j.vetpar.2009.03.02

22. H. J. Bremermann, H. R. R. Thieme, A competitive exclusion principle for pathogen virulence, *J. Math. Biol.*, **27** (1989), 179–190. https://10.1007/BF00276102

23. S. Lion, A. J. J. Metz, Beyond R0 Maximisation: On pathogen evolution and environmental dimensions, *Trends Ecol. Evol.*, **33** (2018), 458–473. https://doi.org/10.1007/s00285-018-1241-y

24. I. Thapa, D. Ghersi, Modeling preferential attraction to infected hosts in vector-borne diseases, *Front. Public Health*, **11** (2023), 1276029. https://doi.org/10.3389/fpubh.2023.1276029

25. H. Zhang, Y. Zhu, Z. Liu, Y. Peng, W. Peng, L. Tong, et al., A volatile from the skin microbiota of flavivirus-infected hosts promotes mosquito attractiveness, *Cell*, **185** (2022), 2510–2522. https://doi.org/10.1016/j.cell.2022.05.016

26. D. W. Vaughn, S. Green, S. Kalayanarooj, B. L. Innis, S. Nimmannitya, S. Suntayakorn, et al., Dengue viremia titer, antibody response pattern, and virus serotype correlate with disease severity, *J. Infect. Dis.*, **181** (2000), 2–9. https://doi.org/10.1086/315215

27. N. Haider, Y. M. Chang, M. Rahman, A. Zumla, R. A. Kock, Dengue outbreaks in Bangladesh: Historic epidemic patterns suggest earlier mosquito control intervention in the transmission season could reduce the monthly growth factor and extent of epidemics, *Curr. Res. Parasitol. Vector-Borne Dis.*, **1** (2021), 100063. https://doi.org/10.1016/j.crpvbd.2021.100063

28. PAHO, Integrated management strategy for dengue prevention and control in the Caribbean subregion, 2010. Available from: https://www.paho.org/sites/default/files/IMS-Dengue%20CARIBBEAN%20SUBREGION%20Integrated%20FINAL.pdf.

29. M. A. Nowak, R. M. May, *Virus Dynamics: Mathematical Principles of Immunology and Virology*, Oxford University Press, 2000.

30. R. Ben-Shachar, K. Koelle, Transmission-clearance trade-offs indicate that dengue virulence evolution depends on epidemiological context, *Nat. Commun.*, **9** (2018), 29907741. https://doi.org/10.1038/s41467-018-04595-w

31. N. J. White, Malaria parasite clearance, *Malar. J.*, **16** (2017). https://doi.org/10.1186/s12936-017-1731-1

32. F. B. Agusto, M. C. Leite, M. E. Orive, The transmission dynamics of a within-and between-hosts malaria model, *Ecol. Complexity*, **38** (2019), 31–55. https://doi.org/10.1016/j.ecocom.2019.02.002

33. J. M. Mansuy, C. Mengelle, C. Pasquier, S. Chapuy-Regaud, P. Delobel, M. B. Guillaume, et al., Zika virus infection and prolonged viremia in whole-blood specimens, *Emerging Infect. Dis.*, **23** (2017), 863–865. https://doi.org/10.3201/eid2305.161631

34. C. Triplett, S. Dufek, N. Niemuth, D. Kobs, C. Cirimotich, K. Mack, et al., Onset and progression of infection based on viral loads in rhesus macaques exposed to Zika virus, *Appl. Microbiol.*, **2** (2022), 544–553. https://doi.org/10.3201/eid2305.161631

35. Y. M. Tun, P. Charunwatthana, C. Duangdee, J. Satayarak, S. Suthisawat, L. Sand, et al., Virological, serological and clinical analysis of Chikungunya virus infection in Thai patients macaques exposed to Zika virus, *Viruses*, **14** (2022), 1805. https://doi.org/10.3390/v14081805

36. M. N. García, R. Hasbun, K. O. Murray, Persistence of West Nile virus, *Microbes Infect.*, **17** (2015), 163–168. https://doi.org/10.1016/j.micinf.2014.12.003

AIMS Press